Research Square

Preprints are preliminary reports that have not undergone peer review.
They should not be considered conclusive, used to inform clinical practice,
or referenced by the media as validated information.

Construction of an Early Recurrence Prediction Model and Real-World Efficacy of Adjuvant Chemoimmunotherapy in High-Risk Biliary Tract Cancer

Jianguo Liao
Sun Yat-sen Memorial Hospital
Xinran Xie
Sun Yat-sen Memorial Hospital
Yin Long
Sun Yat-sen Memorial Hospital
Jue Huang
Sun Yat-sen Memorial Hospital
Lei Zhang
zhangl9@mail.sysu.edu.cn

Sun Yat-sen Memorial Hospital

Research Article

Keywords: Biliary tract cancer, Adjuvant chemoimmunotherapy, Nomogram, Log odds of positive lymph nodes (LODDS), Doubly robust regression, Real-world study

Posted Date: June 30th, 2026

DOI: https://doi.org/10.21203/rs.3.rs-9837235/v1

License: This work is licensed under a Creative Commons Attribution 4.0 International License.
Read Full License

Additional Declarations: No competing interests reported.

Construction of an Early Recurrence Prediction Model and Real-World Efficacy of Adjuvant Chemoimmunotherapy in High-Risk Biliary Tract Cancer

Jianguo Liao[1], Xinran Xie[2], Yin Long[1], Jue Huang[1] and Lei Zhang[1,*]

1 Department of Hepatobiliary Surgery, Sun Yat-sen Memorial Hospital, Sun Yat-sen University, Guangzhou 510120, China; liaojg5@mail2.sysu.edu.cn (J.L.); longy63@mail2.sysu.edu.cn (Y.L.); huangzq39@mail2.sysu.edu.cn (Z.H.);

2 Department of Biliary and Pancreatic Surgery, Sun Yat-sen Memorial Hospital, Sun Yat-sen University, Guangzhou 510120, China; xiexr23@mail2.sysu.edu.cn

Corresponding author： zhangl9@mail.sysu.edu.cn; Tel.: +86-020-3407-0701

Abstract

Background: Despite curative resection, early recurrence of biliary tract cancer (BTC) remains high, and traditional adjuvant chemotherapy has reached a survival benefit bottleneck. Immune checkpoint inhibitors combined with chemotherapy (chemoimmunotherapy) demonstrate breakthrough efficacy in advanced BTC, but high-quality real-world evidence in the postoperative adjuvant setting is lacking. This study aimed to construct an individualized nomogram predicting early recurrence and verify real-world efficacy of adjuvant chemoimmunotherapy.

Methods: This retrospective study enrolled 290 BTC patients with high-risk features who underwent curative resection (January 2015–July 2025). LASSO regression performed dimensionality reduction on high-dimensional clinical features including log odds of positive lymph nodes (LODDS) and systemic immune-inflammation index (SII). A nomogram predicting 1-year and 2-year recurrence-free survival (RFS) was constructed and validated. Patients were stratified into surgery alone (n=94), adjuvant chemotherapy (n=100), and adjuvant chemoimmunotherapy (n=96) groups. IPTW with ATT balanced baseline covariates; doubly robust Cox regression evaluated real-world efficacy.

Results: LASSO identified 9 core features. The nomogram demonstrated good discrimination for 1-year RFS (AUC=0.829) and moderate discrimination for 2-year RFS (AUC=0.709), with high calibration consistency. Decision curve analysis confirmed clinical net benefit. Significant risk stratification was achieved (P<0.001). After IPTW adjustment, adjuvant chemoimmunotherapy significantly reduced 2-year recurrence risk compared to surgery alone (HR=0.466, P=0.002). While chemoimmunotherapy and chemotherapy showed comparable OS improvement, chemoimmunotherapy successfully extended clinical benefit to substantial RFS

improvement. Grade ≥3 adverse events were more frequent with chemoimmunotherapy (12.5% vs. 2.0%), though the safety profile remained manageable.

Conclusions: The Nomogram model, constructed based on multidimensional features such as LODDS and SII, serves as an effective supplement to traditional staging. It can precisely quantify the individual probability of recurrence, providing an objective reference for high-risk triage. For these high-risk populations, adjuvant chemoimmunotherapy is an effective systemic intervention strategy capable of significantly reducing the risk of early postoperative recurrence in BTC.

Keywords: Biliary tract cancer; Adjuvant chemoimmunotherapy; Nomogram; Log odds of positive lymph nodes (LODDS); Doubly robust regression; Real-world study

Background

Biliary tract cancer (BTC) is a highly aggressive and heterogeneous group of malignant solid tumors. Recent global burden studies show that the incidence and mortality of BTC continue to rise , and China faces severe challenges as the country with the heaviest BTC burden worldwide[1]. Although radical resection combined with standardized lymph node dissection is currently the only curative treatment , the postoperative recurrence rate remains extremely high. Studies indicate that even after achieving R0 resection, the estimated 8-year overall recurrence rate for high-risk patients reaches 76%, with a median recurrence-free survival (RFS) of only 26 months.

Furthermore, nearly 40% of patients present with distant metastasis at initial recurrence[2], highlighting the importance of postoperative adjuvant therapy.

Gemcitabine-based adjuvant regimens showed no survival benefit in the BCAT and PRODIGE12 trials[3, 4]. Following the consecutive failures of gemcitabine-based combinations, the BILCAP trial established capecitabine as the cornerstone of standard postoperative adjuvant therapy for BTC[5]. However, the efficacy of chemotherapy alone frequently reaches a bottleneck, with more than half of the patients experiencing disease recurrence or mortality during subsequent follow-up despite receiving standard chemotherapy[6]. As the TOPAZ-1 and KEYNOTE-966 trials have demonstrated survival benefits for immune checkpoint inhibitors (ICIs) combined with chemotherapy in advanced BTC[7, 8], the chemoimmunotherapy regimen has emerged as a novel direction for postoperative intervention. The recent ACCORD phase 2 RCT provided the first prospective evidence that adjuvant PD-1 blockade combined with chemoradiotherapy significantly improved RFS and overall survival (OS) in resected extrahepatic cholangiocarcinoma and gallbladder cancer[9]. However, high-level evidence for adjuvant chemoimmunotherapy remains limited, and real-world data on its efficacy in high-risk BTC patients after curative resection are still scarce, which is the core issue addressed in this study.

Furthermore, the AJCC TNM staging system is susceptible to the "stage migration" phenomenon in BTC, as the complex biliary anatomy frequently precludes adequate lymph node harvest [10, 11]. Although novel biomarkers such as the log odds of positive lymph nodes (LODDS) and the systemic immune-inflammation index (SII) have demonstrated potential for risk [12-14], a single indicator is inadequate to address the demands of multidimensional clinical evaluation. Confronted with high-dimensional clinical data exhibiting multicollinearity, LASSO regression is well-suited for feature extraction and nomogram construction [15]. To address these challenges, this study had two objectives: first, to validate the efficacy of adjuvant chemoimmunotherapy in preventing recurrence among high-risk patients following curative-intent resection for BTC; and second, to develop an individualized nomogram integrating multidimensional biomarkers—including LODDS and SII—for the prediction of early recurrence. This integrated approach aims to provide real-world evidence supporting adjuvant chemoimmunotherapy while equipping clinicians with a quantitative and visualized tool to refine risk stratification and guide tailored postoperative intervention strategies.

Methods

Study Design and Patients

Clinicopathological and follow-up data for patients with biliary tract cancer (BTC) who underwent surgical resection at Sun Yat-sen Memorial Hospital between January 1, 2015, and July 31, 2025, were retrospectively collected. The follow-up cutoff date for this analysis was December 31, 2025.

Patients were considered eligible for inclusion if they met all of the following criteria: (1) histologically confirmed primary BTC, including intrahepatic cholangiocarcinoma (ICC), perihilar cholangiocarcinoma (pCCA), distal cholangiocarcinoma (dCCA), or gallbladder cancer (GBC); (2) pathological staging according to the 8th edition of the AJCC staging manual of pT2–4N0M0 or pT1–4N1–2M0 for extrahepatic BTC and GBC, or pT1–4N0–1M0 for ICC; (3) undergone curative-intent (R0 or R1) resection; and (4) documented presence of at least one high-risk feature, defined as tumor size > 5 cm, microvascular or macrovascular invasion, intrahepatic metastasis or direct invasion of adjacent organs, regional lymph node metastasis, microscopically positive margin (R1) , or preoperative CA 19-9 level > 200 U/mL.

Patients were excluded if they presented with any of the following: (1) distant metastatic disease (M1) or palliative R2 resection; (2) a concurrent diagnosis of another primary or secondary malignancy; (3) atypical histology (e.g., ampullary carcinoma or neuroendocrine neoplasm); (4) prior receipt of neoadjuvant or conversion therapy; or (5) incomplete clinicopathological or follow-up records.

A total of 690 patients who underwent surgical exploration for BTC during the study period were initially screened. Following application of the inclusion and exclusion criteria, 400 patients were excluded for the following reasons: absence of high-risk features (n = 102), non-curative (R2) resection or M1 disease (n = 55), history of concurrent malignancy (n = 22), prior neoadjuvant therapy (n = 90), and atypical pathological findings or incomplete data (n = 131). Consequently, 290 high-risk BTC patients constituted the final analytical cohort.2.2 Data Collection and Definitions

Data were extracted from the institutional electronic medical record (EMR) and laboratory information systems (LIS). Baseline demographic and clinical characteristics included age, sex, hepatitis B surface antigen (HBsAg) status, and the presence of concomitant liver cirrhosis. Preoperative laboratory parameters comprised serum albumin (g/L), carbohydrate antigen 19-9 (CA 19-9, U/mL), and the systemic immune-inflammation index (SII), which was calculated as SII = (platelet count × neutrophil count) / lymphocyte count. Surgical and histopathological features documented for each case included surgical approach, maximal tumor diameter (cm), tumor multiplicity (solitary vs. multiple), tumor differentiation (well/moderate vs. poor/undifferentiated), resection margin status (R0 vs. R1), pathological T stage (pT1–2 vs. pT3–4), and lymph node status (N0 vs. N1–2). To further quantify the extent of nodal involvement, the log odds of positive lymph nodes (LODDS) was computed using the following formula: LODDS = ln [(PLN + 0.5) / (TLN - PLN + 0.5)], where PLN denotes the number of positive lymph nodes and TLN represents the total number of lymph nodes examined.

Treatment Protocol

Based on the specific postoperative adjuvant regimen administered following curative-intent resection, the 290 high-risk patients were stratified into three comparative cohorts. The surgery-alone cohort comprised 94 patients who did not receive any systemic antineoplastic therapy postoperatively and underwent routine surveillance only. The adjuvant chemotherapy cohort included 100 patients treated exclusively with standard postoperative systemic chemotherapy, consisting of either single-agent capecitabine or S-1, or doublet regimens such as gemcitabine plus oxaliplatin or cisplatin. The adjuvant chemoimmunotherapy cohort consisted of 96 patients who received a combination of standard chemotherapy and immune checkpoint blockade with anti–PD-1 or anti–PD-L1 monoclonal antibodies.

Follow-up and outcomes

Patients were followed every 3 months for the first 2 postoperative years, every 6 months from years 3 to 5, and annually thereafter. The median follow-up time was calculated using the reverse Kaplan-Meier method based on overall survival**.** Routine assessments included physical examination, complete blood count, liver and kidney function tests, serum tumor markers (CA 19-9 and CEA), and contrast-enhanced abdominal CT or MRI; whole-body PET-CT or bone scintigraphy was performed when clinically indicated to exclude distant metastasis.

The primary endpoint was recurrence-free survival (RFS), defined as the time from curative-intent surgery to first confirmed recurrence (locoregional or distant) by imaging or biopsy. Patients who died from any cause without prior recurrence were censored at the time of death. Overall survival (OS) was the secondary endpoint, defined as the time from surgery to death from any cause. Patients alive and recurrence-free at the data cutoff were censored at the last follow-up visit.

Statistical Analysis

All statistical analyses were performed using R software, version 4.3.2 (R Foundation for Statistical Computing, Vienna, Austria). Continuous variables are expressed as mean ± SD or median (IQR) and were compared using the Student t-test or Mann-Whitney *U* test, as appropriate; categorical variables are presented as frequencies (percentages) and were compared using the χ^2 test or Fisher exact test. Survival curves were estimated by the Kaplan-Meier method and compared with the log-rank test. To address high-dimensional data and mitigate overfitting, LASSO Cox regression with 5-fold cross-validation was employed for feature selection. The optimal tuning parameter λ was determined by minimizing the cross-validated partial log-likelihood deviance (λ.min = 0.051, log(λ.min) = −2.976). Variables with non-zero coefficients at the optimal λ were retained for subsequent multivariate Cox regression and nomogram construction. Internal validation was performed with 1,000 bootstrap resamples to correct for optimism, with discrimination assessed via time-dependent AUC, calibration via bias-corrected calibration plots, and clinical utility via decision curve analysis. Optimal cut-offs were derived to define risk strata. To address indication bias, IPTW with ATT weights was applied; covariate balance was assessed using SMD (threshold ≤ 0.15). A doubly robust Cox model incorporating ATT weights and key baseline covariates was fitted to estimate treatment effect HRs with 95% CIs. To assess

the robustness of the ATT-based estimates to the choice of weighting strategy, a pre-specified sensitivity analysis was performed using average treatment effect on the overlap (ATO) weights, which restrict the estimand to the region of clinical equipoise and are less susceptible to extreme propensity score weights. All tests were two-sided, with $P \leq .05$ considered statistically significant.

Results

Baseline Characteristics

A total of 290 patients with high-risk biliary tract cancer (BTC) were included, of whom 137 (47.2%) experienced disease recurrence during follow-up. The median follow-up time was 25.7 months (95% CI, 21.9–31.9), and the 1-year and 2-year RFS rates for the entire cohort were 68.3% (95% CI, 62.4%–74.6%) and 43.5% (95% CI, 36.7%–51.6%), respectively. The overall cohort exhibited aggressive clinicopathological features, with 55.5% having pT3–T4 disease, 44.5% microvascular invasion, 38.3% poorly differentiated or undifferentiated tumors, and 50.3% lymph node metastasis. The median SII was 761.6, and the median CA 19-9 level was 174.4 U/ml. (Table 1).

Table 1 Baseline Characteristics of the Study Cohort Stratified by

208 **Recurrence Status.**

Variables	Total Cohort	Recurrence-free	Recurrence	*P*
Participants (n)	290	153	137	
Demographics and Clinical Characteristics				
Age (yr)	62.1 ± 10.3	63.5 ± 9.5	60.4 ± 11.0	0.010
Female, n (%)	135 (46.6)	79 (51.6)	56 (40.9)	0.067
HBsAg status	46 (15.9)	21 (13.7)	25 (18.2)	0.293
Liver cirrhosis	16 (5.5)	7 (4.6)	9 (6.6)	0.458
Hepatolithiasis	103 (35.5)	51 (33.3)	52 (38)	0.412
Preoperative biliary drainage	118 (40.7)	66 (43.1)	52 (38)	0.37
Preoperative Laboratory Parameters				
CA 19-9, U/mL, median (IQR)	174.4 (32.5, 686.8)	140.3 (26.3, 652.0)	215.0 (48.8, 763.2)	0.246
CEA, ng/mL, median (IQR)	3.5 (2.0, 6.4)	3.2 (1.7, 5.8)	3.8 (2.2, 7.3)	0.089
Systemic immune-inflammation index, median (IQR)	761.6 (497.9, 1201.3)	727.6 (497.0, 1115.2)	785.8 (500.6, 1376.9)	0.281
Total bilirubin, μmol/L	35.9 (12.8, 106.2)	37.1 (13.8, 84.8)	30.5 (12.7, 125.0)	0.911
Albumin, g/L, mean ± SD	36.4 ± 5.0	36.4 ± 5.0	36.4 ± 4.9	0.918

Tumor and Pathological Characteristics				
Tumor location				0.031
Gallbladder carcinoma	63 (21.7)	24 (15.7)	39 (28.5)	
Hilar cholangiocarcinoma	132 (45.5)	79 (51.6)	53 (38.7)	
Intrahepatic cholangiocarcinoma	51 (17.6)	29 (19)	22 (16.1)	
Distal cholangiocarcinoma	44 (15.2)	21 (13.7)	23 (16.8)	
Tumor multiplicity	63 (21.7)	26 (17)	37 (27)	0.039
Tumor size, cm	3.6 ± 2.2	3.5 ± 2.0	3.8 ± 2.5	0.232
Differentiation grade				0.021
Poor to undifferentiated	111 (38.3)	49 (32)	62 (45.3)	
Well to moderate	179 (61.7)	104 (68)	75 (54.7)	
Macrovascular invasion	87 (30.0)	47 (30.7)	40 (29.2)	0.778
Microvascular invasion (MVI)	129 (44.5)	66 (43.1)	63 (46)	0.626
Perineural invasion (PNI)	198 (68.3)	104 (68)	94 (68.6)	0.907
pT stage				0.351
T1-T2	129 (44.5)	72 (47.1)	57 (41.6)	

T3-T4	161 (55.5)	81 (52.9)	80 (58.4)	
Lymph node metastasis	146 (50.3)	72 (47.1)	74 (54)	0.237
LODDS, median (IQR)	-1.6 (-2.7, -0.4)	-1.8 (-2.8, -0.6)	-1.5 (-2.4, -0.2)	0.035
Surgical Outcomes and Complications				
Surgical procedure				0.139
Extrahepatic bile duct resection	35 (12.1)	23 (15)	12 (8.8)	
Hepatectomy with bile duct resection	209 (72.1)	110 (71.9)	99 (72.3)	
Pancreaticoduodenectomy	46 (15.9)	20 (13.1)	26 (19)	
Resection margin (R1)	71 (24.5)	34 (22.2)	37 (27)	0.344
Postoperative bile leak	60 (20.7)	38 (24.8)	22 (16.1)	0.065
Postoperative infection	70 (24.1)	43 (28.1)	27 (19.7)	0.095
Adjuvant therapy				0.013
Surgery alone	94 (32.4)	47 (30.7)	47 (34.3)	
Adjuvant chemotherapy	100 (34.5)	44 (28.8)	56 (40.9)	
Adjuvant chemoimmunotherapy	96 (33.1)	62 (40.5)	34 (24.8)	

209 Data are presented as mean ± SD, median (IQR), or n (%). P values were derived from
210 the Student t-test, Mann-Whitney U test, χ^2 test, or Fisher's exact test as appropriate.

Abbreviations: HBsAg, hepatitis B surface antigen; CA 19-9, carbohydrate antigen 19-9; IQR, interquartile range; CEA, carcinoembryonic antigen; SII, systemic immune-inflammation index; SD, standard deviation; MVI, microvascular invasion; PNI, perineural invasion; LODDS, log odds of positive lymph nodes; pT, pathological tumor stage.

Compared with patients without recurrence, those who recurred were significantly younger (mean age, 60.4 vs. 63.5 years; P = .010), had higher rates of multifocal tumors (27.0% vs. 17.0%; P = .039) and poorly differentiated/undifferentiated histology (45.3% vs. 32.0%; P = .021), and demonstrated a greater nodal disease burden (median LODDS, −1.5 vs. −1.8; P = .035). Significant differences were also noted in primary tumor site distribution (P = .031) and adjuvant treatment modality (P = .013).

Feature Selection and Prognostic Factors

Sixteen clinically relevant candidate variables were entered into the predictive modeling analysis. LASSO regression with 5-fold cross-validation identified nine core variables associated with RFS: tumor multiplicity, tumor size, histologic grade, resection margin status, LODDS, SII, preoperative albumin, CA 19-9 level, and adjuvant therapeutic strategy (Figure 1).

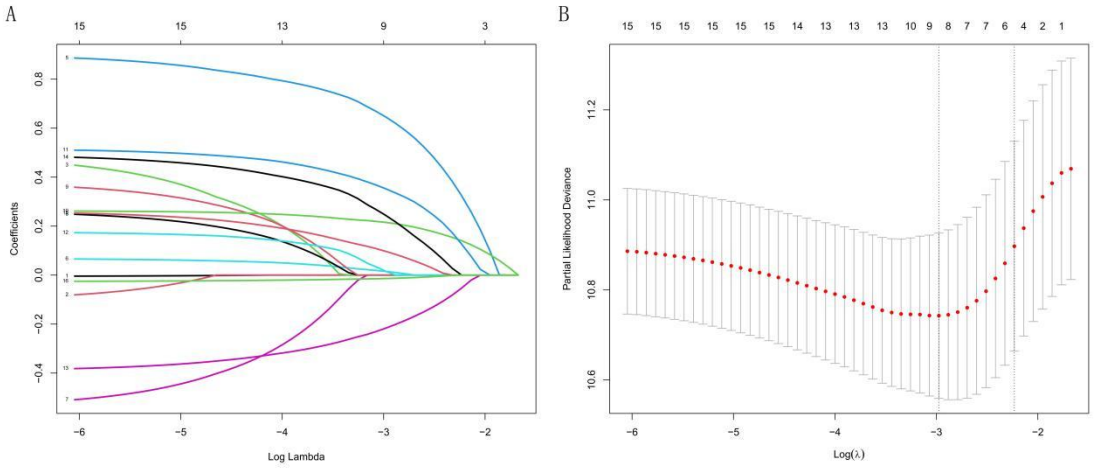


Figure 1 Feature selection using the LASSO regression algorithm. A LASSO coefficient profiles of the candidate clinical features. **B** Five-fold cross-validation for tuning parameter selection in the LASSO model. The solid vertical lines represent the optimal values based on the minimum criteria and the 1-standard error of the minimum criteria. *Abbreviations:* LASSO, least absolute shrinkage and selection operator.

Multivariable Cox regression demonstrated that tumor multiplicity (HR = 2.52; 95% CI, 1.68–3.78; P < .001), poorly differentiated/undifferentiated histology (HR = 1.67; 95% CI, 1.16–2.39; P = .005), CA 19-9 ≥ 37 U/mL (HR = 1.71; 95% CI, 1.12–2.61; P = .013), and higher LODDS (HR = 1.30; 95% CI, 1.14–1.47; P < .001) were independent risk factors for worse RFS, whereas adjuvant chemoimmunotherapy (HR = 0.48; 95% CI, 0.31–0.75; P = .001) was an independent protective factor (Table 2). Although tumor size, resection margin status, albumin, and SII did not achieve

245 statistical significance in the multivariable model, they were retained in the final

246 nomogram given their non-zero LASSO coefficients, contribution to predictive

247 variance, and established clinical relevance.

248

249 **TABLE 2. Univariable and multivariable Cox proportional hazards analysis**

250 **of factors associated with recurrence-free survival (RFS).**

	Univariate		Multivariable Analysis	
	HR (95% CI)	***P* value**	**HR (95% CI)**	***P* value**
Age (yr)	1.0028 (0.9873,1.0186)	0.722		
Sex (Male vs. Female)	0.8 (0.57,1.13)	0.203		
HBsAg status	1.21 (0.79,1.87)	0.38		
Liver cirrhosis	1.22 (0.62,2.41)	0.559		
Hepatolithiasis	1.59 (1.12,2.26)	0.009		
Preoperative biliary drainage	0.89 (0.63,1.26)	0.524		
CA 19-9, U/mL				
<37	Reference			
≥37	1.65 (1.1,2.46)	0.015	1.71 (1.12,2.61)	0.013
CEA, ng/mL				
<5	Reference			
≥5	1.6 (1.13,2.27)	0.008		
Systemic immune-inflammation index				
<500	Reference		Reference	
500-1200	1.11 (0.73,1.7)	0.619	1.09 (0.71,1.67)	0.706
≥1200	1.74 (1.11,2.75)	0.017	1.52 (0.95,2.44)	0.084
Total bilirubin, μmol/L				
<21	Reference			
≥21	0.73 (0.52,1.02)	0.065		

Albumin, g/L	0.96 (0.93,0.99)	0.009	0.97 (0.94,1.01)	0.147
Tumor location				
Gallbladder carcinoma	Reference			
Hilar cholangiocarcinoma	0.51 (0.33,0.77)	0.001		
Intrahepatic cholangiocarcinoma	0.7 (0.41,1.18)	0.176		
Distal cholangiocarcinoma	0.74 (0.44,1.24)	0.258		
Tumor multiplicity	2.53 (1.71,3.73)	< 0.001	2.52 (1.68,3.78)	<0.001
Tumor size, cm	1.07 (1,1.15)	0.037	1.06 (0.99,1.15)	0.104
Differentiation grade				
Well to moderate	Reference			
Poor to undifferentiated	1.83 (1.31,2.56)	< 0.001	1.67 (1.16,2.39)	0.005
Macrovascular invasion	0.88 (0.61,1.28)	0.506		
Microvascular invasion (MVI)	1.21 (0.86,1.69)	0.271		
Perineural invasion (PNI)	1.08 (0.75,1.55)	0.686		
pT stage				
T1-T2	Reference			
T3-T4	1.15 (0.82,1.62)	0.407		
Lymph node metastasis	1.49 (1.06,2.09)	0.02		
LODDS	1.39 (1.23,1.57)	< 0.001	1.3 (1.14,1.47)	<0.001
Surgical procedure				
Extrahepatic bile duct resection	Reference			
Hepatectomy with bile duct resection	0.65 (0.35,1.18)	0.154		
Pancreaticoduodenectomy	1.22 (0.79,1.89)	0.362		
Resection margin (R1 vs. R0)	1.49 (1.02,2.17)	0.039	1.2 (0.79,1.83)	0.392
Postoperative bile leak	0.63 (0.4,1)	0.048		
Postoperative infection	0.87 (0.57,1.33)	0.525		
Adjuvant therapy				
Surgery alone	Reference		Reference	
Adjuvant Chemotherapy	0.73 (0.49,1.08)	0.114	0.87 (0.58,1.31)	0.506

Immuno-Chemo	0.49 (0.31,0.76)	0.002		0.48 (0.31,0.75)	0.001

The multivariable model included only variables selected by the LASSO regression algorithm. HRs with 95% CIs and P values are reported.

Abbreviations: HR, hazard ratio; CI, confidence interval; RFS, recurrence-free survival; HBsAg, hepatitis B surface antigen; CA 19-9, carbohydrate antigen 19-9; CEA, carcinoembryonic antigen; SII, systemic immune-inflammation index; MVI, microvascular invasion; PNI, perineural invasion; LODDS, log odds of positive lymph nodes; pT, pathological tumor stage; Immuno-Chemo, adjuvant chemoimmunotherapy.

Construction and Validation of the Nomogram And Risk Subgroup Classification

Based on the nine variables identified by LASSO regression, an individualized nomogram was constructed to predict 1- and 2-year recurrence-free survival (RFS) in high-risk BTC patients (Figure 2). The model integrates tumor-related pathological features (multiplicity, size, histologic grade, margin status, and LODDS), host systemic status (SII, albumin, CA 19-9), and adjuvant treatment modality to provide a quantitative risk assessment.

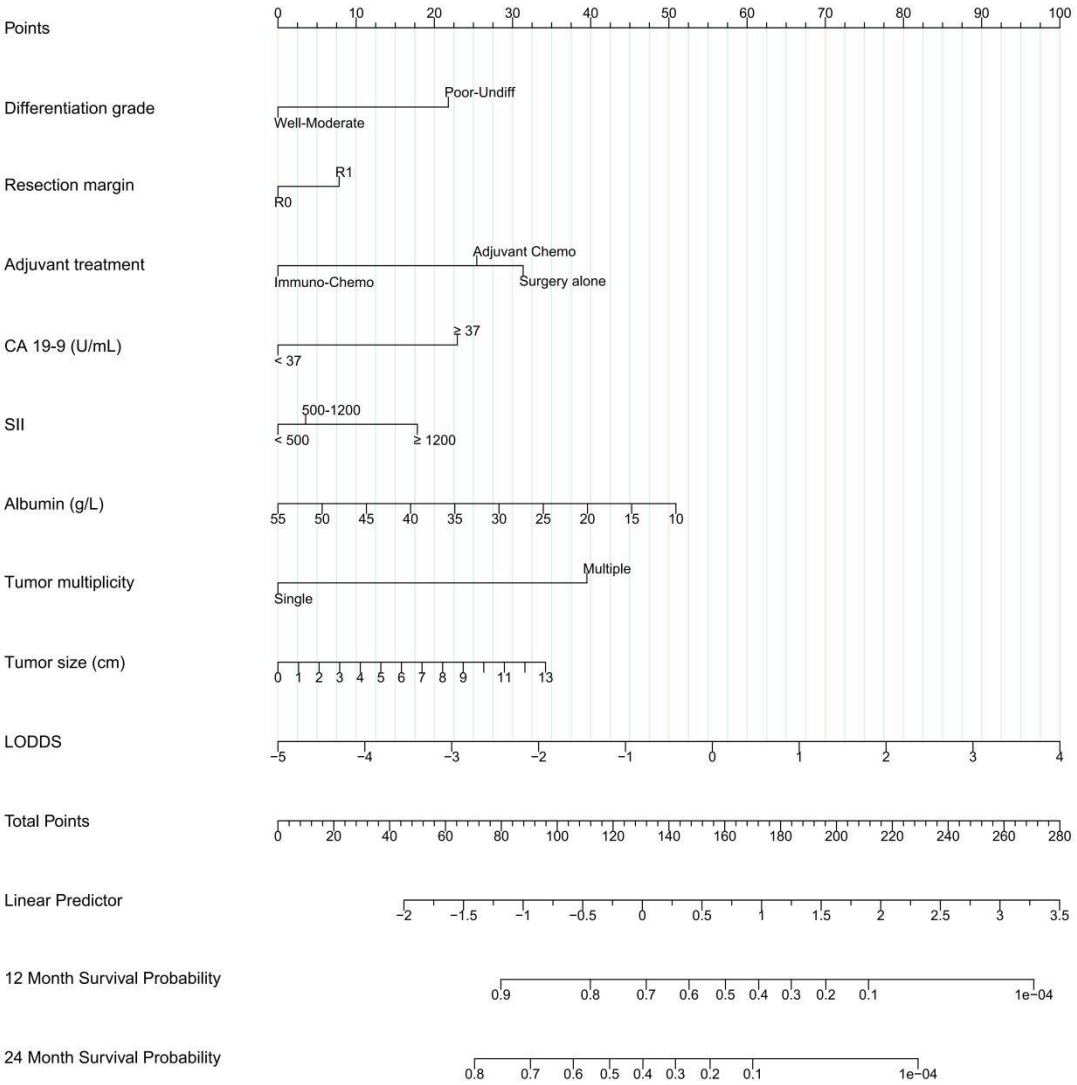


Figure 2 Nomogram for predicting 1-year and 2-year recurrence-free survival.

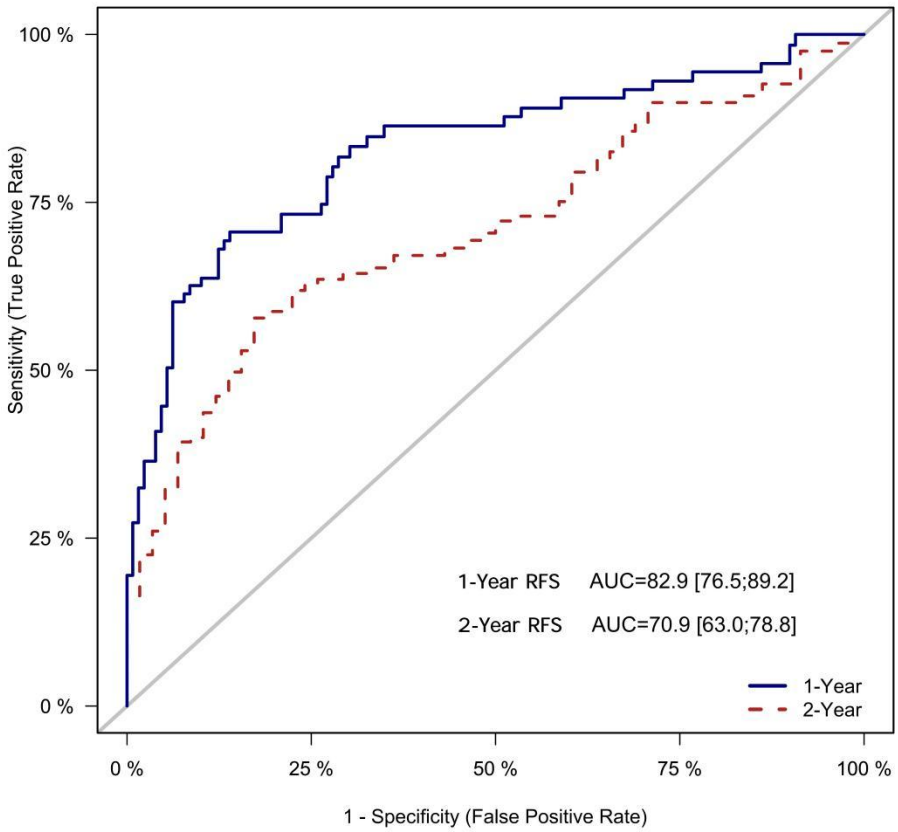
The individualized nomogram was constructed based on the nine core variables identified by LASSO regression. *Abbreviations:* RFS, recurrence-free survival; LODDS, log odds of positive lymph nodes; SII, systemic immune-inflammation index; CA 19-9, carbohydrate antigen 19-9; Chemo, adjuvant chemotherapy; Immuno-Chemo, adjuvant chemoimmunotherapy.

Rigorous internal validation was performed across three domains. First, discrimination was assessed using time-dependent receiver operating characteristic (ROC) curves. The area under the curve (AUC) for predicting 1-year RFS was 0.829 (95% CI, 0.765–0.892), indicating good discriminative performance, and the AUC for 2-year RFS was 0.709 (95% CI, 0.630–0.788), indicating moderate discriminative performance. (Figure 3). Second, bias-corrected calibration curves derived from 1,000 bootstrap resamples demonstrated strong agreement between nomogram-predicted and observed recurrence probabilities, with no evidence of systematic overestimation or underestimation (Figure 4A, B). Third, decision curve analysis (DCA) revealed that across a wide range of threshold probabilities (12%–98% for 1-year RFS; 40%–89% for 2-year RFS), the nomogram-guided strategy yielded a greater net clinical benefit than either the "treat-all" or "treat-none" approach, supporting its clinical utility (Figure 4C, D).

To further evaluate the clinical stratification capacity of the nomogram, patients were divided into high-risk (n = 145) and low-risk (n = 145) subgroups using the median nomogram score as the cutoff. The risk distribution plot (Figure 5A) visually depicts the association between individual risk scores and survival outcomes, showing a clear increase in the proportion of recurrence events with higher scores. Kaplan-Meier

295 survival analysis confirmed a statistically significant difference in RFS between the

296 two risk strata (log-rank $P < .001$; Figure 5B).



297

298 **Figure 3 Time-dependent ROC curves of the predictive model.** Discriminative

299 performance of the nomogram for predicting 1-year and 2-year recurrence-free

300 survival in the high-risk BTC cohort. *Abbreviations:* ROC, receiver operating

301 characteristic; AUC, area under the curve; RFS, recurrence-free survival.

302

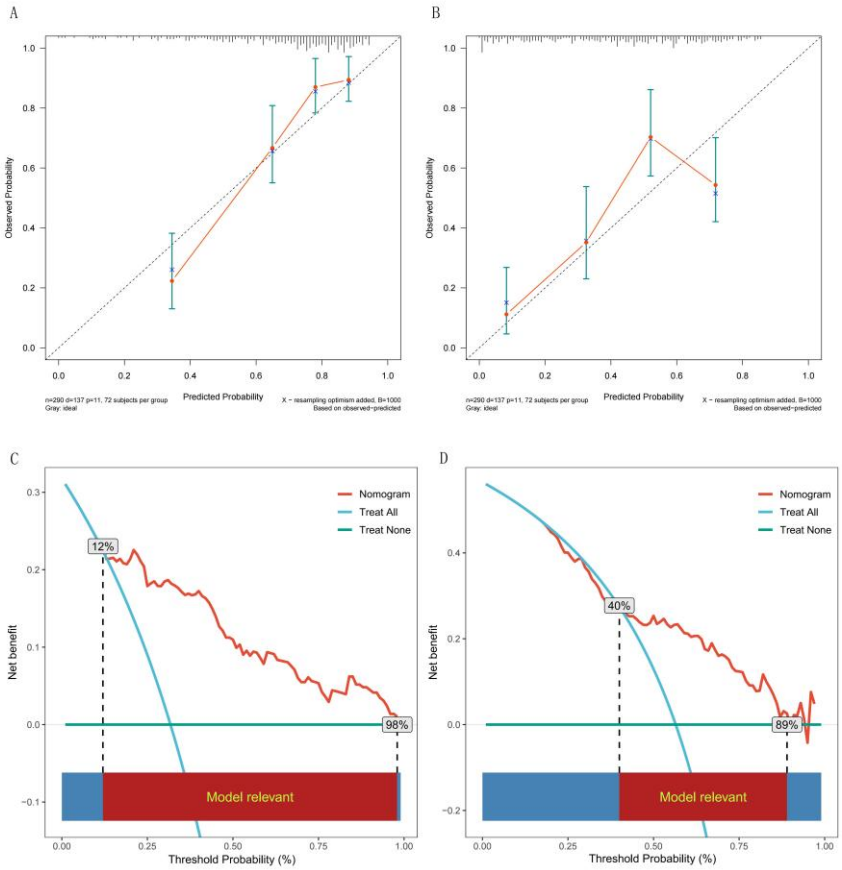
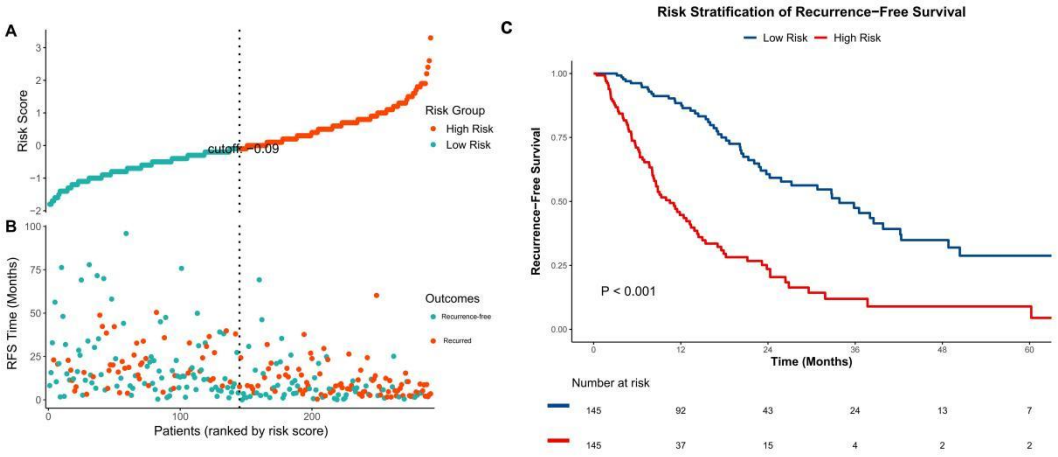


Figure 4 Calibration curves and decision curve analysis of the nomogram. A, B Bias-corrected calibration curves for predicting 1-year (**A**) and 2-year (**B**) RFS. The diagonal dashed line represents the ideal prediction, and the solid line represents the actual nomogram performance. **C, D** Decision curve analysis (DCA) for 1-year (**C**) and 2-year (**D**) RFS, demonstrating the net clinical benefit across a wide range of threshold probabilities. *Abbreviations:* RFS, recurrence-free survival; DCA, decision curve analysis.



311

312 **Figure 5 Risk stratification and survival analysis based on nomogram scores. A**

313 The distribution of nomogram risk scores, recurrence status, and survival time. The

314 dotted vertical line represents the median cutoff value dividing patients into high-risk

315 and low-risk subgroups. **B** Kaplan-Meier survival curves comparing recurrence-free

316 survival between the high-risk and low-risk subgroups. The P value was calculated

317 using the log-rank test. *Abbreviations:* RFS, recurrence-free survival.

318

319

320 An interactive web-based version of this nomogram for point-of-care use is available

321 at https://liaojianguo.shinyapps.io/DynNom_Cox_model. This nomogram-based risk

322 stratification provided the foundation for evaluating whether adjuvant

323 chemoimmunotherapy could modify the early recurrence risk in this high-risk

324 population.

325 **Baseline Balance After IPTW Adjustment**

Although the risk stratification model identified a subset of patients at elevated risk, comparing the real-world effectiveness of different adjuvant regimens requires addressing the selection bias inherent in retrospective cohort studies. Accordingly, prior to evaluating differences in efficacy among adjuvant chemoimmunotherapy, adjuvant chemotherapy, and surgery alone, inverse probability of treatment weighting (IPTW) was applied to balance baseline covariates across the three treatment groups. In the unweighted cohort, substantial imbalances were observed for several key prognostic variables, including preoperative CA 19-9 level, the systemic immune-inflammation index (SII), and log odds of positive lymph nodes (LODDS), with standardized mean differences (SMDs) exceeding 0.15 (Table 3).

TABLE 3. Baseline Characteristics of High-Risk Patients Before and After IPTW (ATT) Adjustment

Variables	Unadjusted Cohort				ATT-Adjusted Cohort			
	Surgery alone	Adjuvant Chemotherapy	Immuno-Chemo	*P*	Surgery alone	Adjuvant Chemotherapy	Immuno-Chemo	SMD
Participants (n)	94	100	96		88.8	93.4	96.0	
ESS					43.2	43.3	96	
Demographics and Clinical Characteristics								
Age (yr)	65.6 ± 10.3	60.0 ± 10.0	60.8 ± 9.9	< 0.01	60.6 ± 10.1	61.7 ± 9.2	60.8 ± 9.9	0.075

Female, n (%)	46 (48.9)	41 (41)	48 (50)	0.384	42.9 (48.3)	41.5 (44.4)	48.0 (50.0)	0.075
HBsAg status	12 (12.8)	19 (19)	15 (15.6)	0.492	14.7 (16.6)	16.0 (17.1)	15.0 (15.6)	0.026
Liver cirrhosis	4 (4.3)	7 (7)	5 (5.2)	0.695	2.8 (3.1)	3.6 (3.9)	5.0 (5.2)	0.070
Hepatolithiasis	48 (51.1)	23 (23)	32 (33.3)	< 0.01	42.8 (48.2)	33.1 (35.5)	32.0 (33.3)	0.204
Preoperative biliary drainage	36 (38.3)	43 (43)	39 (40.6)	0.801	40.4 (45.5)	35.4 (37.9)	39.0 (40.6)	0.103
Preoperative Laboratory Parameters								
CA 19-9, U/mL, median (IQR)	254.0 (27.6, 1347.5)	159.1 (29.1, 462.8)	140.2 (43.1, 618.6)	0.188	176.6 (19.6, 555.3)	218.2 (39.7, 769.3)	140.0 (41.4, 609.0)	0.095
CEA, ng/mL, median (IQR)	3.7 (2.2, 7.2)	2.9 (2.0, 5.6)	3.5 (1.9, 6.4)	0.342	3.7 (2.3, 5.6)	3.0 (1.7, 7.3)	3.5 (1.9, 6.4)	0.031
Systemic immune-inflammation index, median (IQR)	792.3 (495.4, 1398.3)	770.4 (511.8, 1267.5)	716.2 (470.8, 1128.4)	0.683	792.9 (428.1, 1381.7)	752.2 (454.2, 1090.1)	710.9 (465.8, 1125.8)	0.111
Total bilirubin, μmol/L	29.4 (11.2, 121.6)	45.9 (15.7, 141.7)	31.1 (13.7, 68.0)	0.053	29.3 (9.9, 85.4)	26.9 (12.2, 57.3)	30.7 (13.3, 67.1)	0.029
Albumin, g/L, mean ± SD	35.6 ± 5.5	37.0 ± 4.4	36.6 ± 5.0	0.124	35.3 ± 7.0	36.4 ± 3.9	36.6 ± 5.0	0.141
Tumor and Pathological Characteristics								
Tumor location				0.096				0.199
Gallbladder carcinoma	25 (26.6)	22 (22)	16 (16.7)		19.2 (21.6)	13.7 (14.6)	16.0 (16.7)	

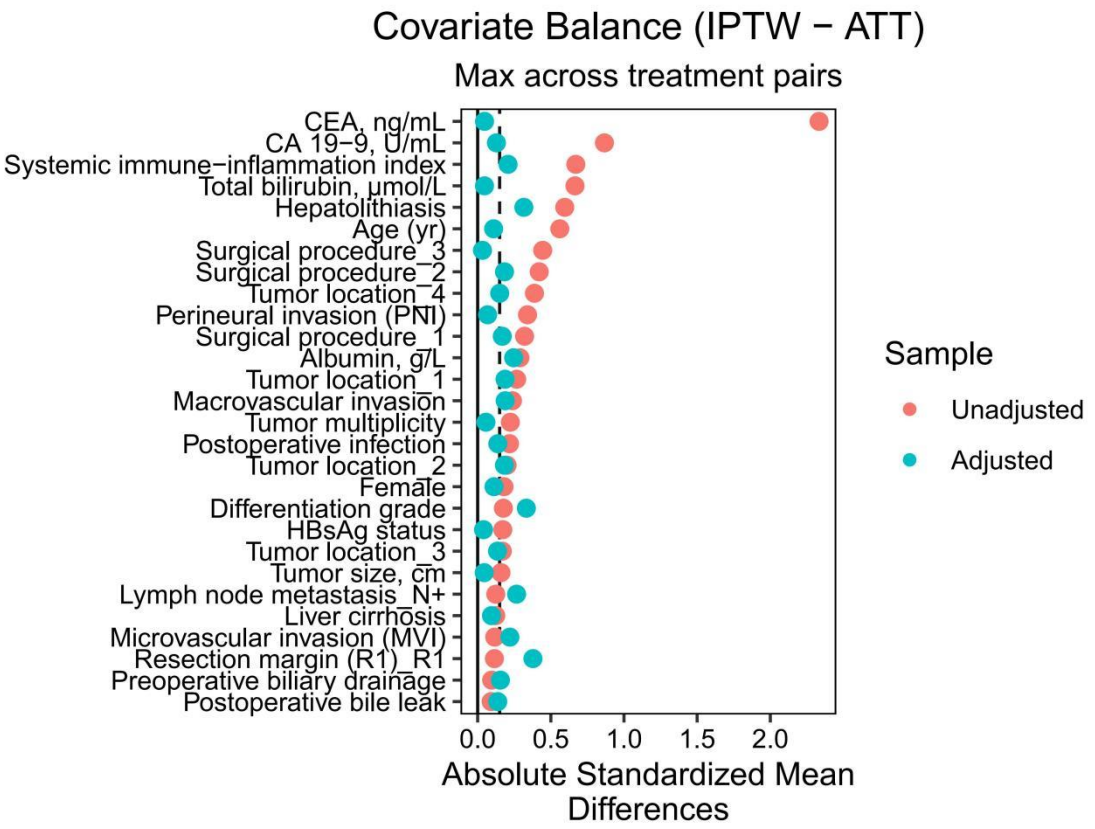
Hilar cholangiocarcinoma	42 (44.7)	41 (41)	49 (51)		37.2 (41.9)	45.0 (48.2)	49.0 (51.0)	
Intrahepatic cholangiocarcinoma	17 (18.1)	14 (14)	20 (20.8)		18.0 (20.2)	24.1 (25.8)	20.0 (20.8)	
Distal cholangiocarcinoma	10 (10.6)	23 (23)	11 (11.5)		14.4 (16.2)	10.7 (11.4)	11.0 (11.5)	
Tumor multiplicity	24 (25.5)	16 (16)	23 (24)	0.222	22.4 (25.3)	24.6 (26.4)	23.0 (24.0)	0.037
Tumor size, cm	3.7 ± 2.4	3.4 ± 2.1	3.7 ± 2.2	0.486	3.6 ± 2.4	3.7 ± 2.4	3.7 ± 2.2	0.028
Differentiation grade				0.471				0.224
Poor to undifferentiated	40 (42.6)	34 (34)	37 (38.5)		27.2 (30.7)	43.8 (46.9)	37.0 (38.5)	
Well to moderate	54 (57.4)	66 (66)	59 (61.5)		61.6 (69.3)	49.6 (53.1)	59.0 (61.5)	
Macrovascular invasion	25 (26.6)	26 (26)	36 (37.5)	0.146	32.4 (36.5)	26.5 (28.4)	36.0 (37.5)	0.130
Microvascular invasion (MVI)	44 (46.8)	41 (41)	44 (45.8)	0.681	45.2 (51.0)	37.4 (40.0)	44.0 (45.8)	0.147
Perineural invasion (PNI)	59 (62.8)	65 (65)	74 (77.1)	0.072	65.9 (74.2)	70.6 (75.6)	74.0 (77.1)	0.044
pT stage				0.428				0.288
T1-T2	46 (48.9)	45 (45)	38 (39.6)		32.3 (36.4)	53.7 (57.5)	38.0 (39.6)	
T3-T4	48 (51.1)	55 (55)	58 (60.4)		56.5 (63.6)	39.7 (42.5)	58.0 (60.4)	
Lymph node metastasis	50 (53.2)	47 (47)	49 (51)	0.68	43.0 (48.5)	35.3 (37.8)	49.0 (51.0)	0.180

LODDS, median (IQR)	-1.43 (-2.38, 0.00)	-1.89 (-2.72, -0.78)	-1.61 (-2.71, -0.43)	0.165	-1.61 (-2.71, -0.51)	-1.95 (-2.83, -1.10)	-1.61 (-2.71, -0.45)	0.118
Surgical Outcomes and Complications								
Surgical procedure				< 0.01				0.136
Extrahepatic bile duct resection	6 (6.4)	6 (6)	23 (24)		14.3 (16.1)	18.7 (20.1)	23.0 (24.0)	
Hepatectomy with bile duct resection	76 (80.9)	70 (70)	63 (65.6)		65.3 (73.6)	64.2 (68.7)	63.0 (65.6)	
Pancreaticoduodenectomy	12 (12.8)	24 (24)	10 (10.4)		9.1 (10.2)	10.5 (11.2)	10.0 (10.4)	
Resection margin (R1)	23 (24.5)	22 (22)	26 (27.1)	0.71	30.0 (33.8)	15.9 (17.0)	26.0 (27.1)	0.261
Postoperative bile leak	21 (22.3)	21 (21)	18 (18.8)	0.826	11.9 (13.4)	12.8 (13.7)	18.0 (18.8)	0.097
Postoperative infection	26 (27.7)	18 (18)	26 (27.1)	0.207	18.6 (21.0)	21.0 (22.5)	26.0 (27.1)	0.096

Standardized mean differences (SMDs) were used to assess covariate balance; SMD ≤ 0.15 was considered acceptable. ESS denotes effective sample size, calculated as $(\sum w)^2 / \sum w^2$.

Abbreviations: IPTW, inverse probability of treatment weighting; ATT, average treatment effect on the treated; SMD, standardized mean difference; ESS, effective sample size; SD, standard deviation; IQR, interquartile range; HBsAg, hepatitis B surface antigen; CA 19-9, carbohydrate antigen 19-9; CEA, carcinoembryonic antigen; SII, systemic immune-inflammation index; MVI, microvascular invasion; PNI, perineural invasion; LODDS, log odds of positive lymph nodes; Immuno-Chemo, adjuvant chemoimmunotherapy.

Using an IPTW model based on average treatment effect on the treated (ATT) weights, the SMDs for the vast majority of critical covariates were reduced to within the predefined acceptable threshold of 0.15 (Figure 6). For example, the SMDs for age, female sex, and HBsAg positivity decreased to 0.075, 0.075, and 0.026, respectively, and the SMD for LODDS was reduced to 0.118. However, this covariate balance was achieved at the cost of reduced effective sample sizes in the two non-target groups, with ESS values of 43.2 (surgery alone), 43.3 (adjuvant chemotherapy), and 96 (adjuvant chemoimmunotherapy), respectively (Table 3). Of note, residual imbalance persisted for hepatolithiasis (SMD = 0.204) and pT stage (SMD = 0.288), reflecting the inherent difficulty of fully balancing all baseline characteristics in a modestly sized real-world cohort. These results indicated that IPTW effectively mitigated baseline discrepancies among the groups, achieving adequate covariate balance across the three cohorts with respect to core clinicopathological characteristics. This established a robust foundation for the subsequent objective evaluation of treatment effects within a pseudo-randomized analytic framework (Table 3).



366

367 **Figure 6 Covariate balance before and after IPTW adjustment.** The plot

368 illustrates the standardized mean differences (SMDs) for baseline covariates across

369 the three treatment cohorts before (unadjusted) and after (ATT-adjusted) inverse

370 probability of treatment weighting. The dashed vertical line at an SMD of 0.15

371 indicates the predefined threshold for an acceptable covariate balance. *Abbreviations:*

372 IPTW, inverse probability of treatment weighting; ATT, average treatment effect on

373 the treated; SMD, standardized mean difference; LODDS, log odds of positive lymph

374 nodes; SII, systemic immune-inflammation index.

375

376 **Doubly Robust Evaluation of Efficacy**

Within the IPTW-balanced cohort, a doubly robust Cox regression model was fitted to evaluate the independent association between adjuvant treatment strategy and survival outcomes. The doubly robust model adjusted for pre-specified covariates, including age, histologic grade, resection margin, lymph node status, and the principal determinants of pathological T stage (tumor multiplicity, tumor size, macrovascular invasion, and microvascular invasion).

Doubly robust estimation revealed that, compared with surgery alone, adjuvant chemotherapy was not associated with a significant reduction in recurrence risk, either for overall RFS (HR = 0.884; 95% CI, 0.516–1.510; *P* = .652) or for 2-year RFS (HR = 0.774; 95% CI, 0.437–1.370; *P* = .378). In contrast, adjuvant chemoimmunotherapy conferred a significant reduction in overall recurrence risk (HR = 0.505; 95% CI, 0.315–0.812; *P* = .005) and was associated with a 53.4% lower risk of recurrence at 2 years relative to surgery alone (HR = 0.466; 95% CI, 0.286–0.758; *P* = .002) (Figures 7A–D).

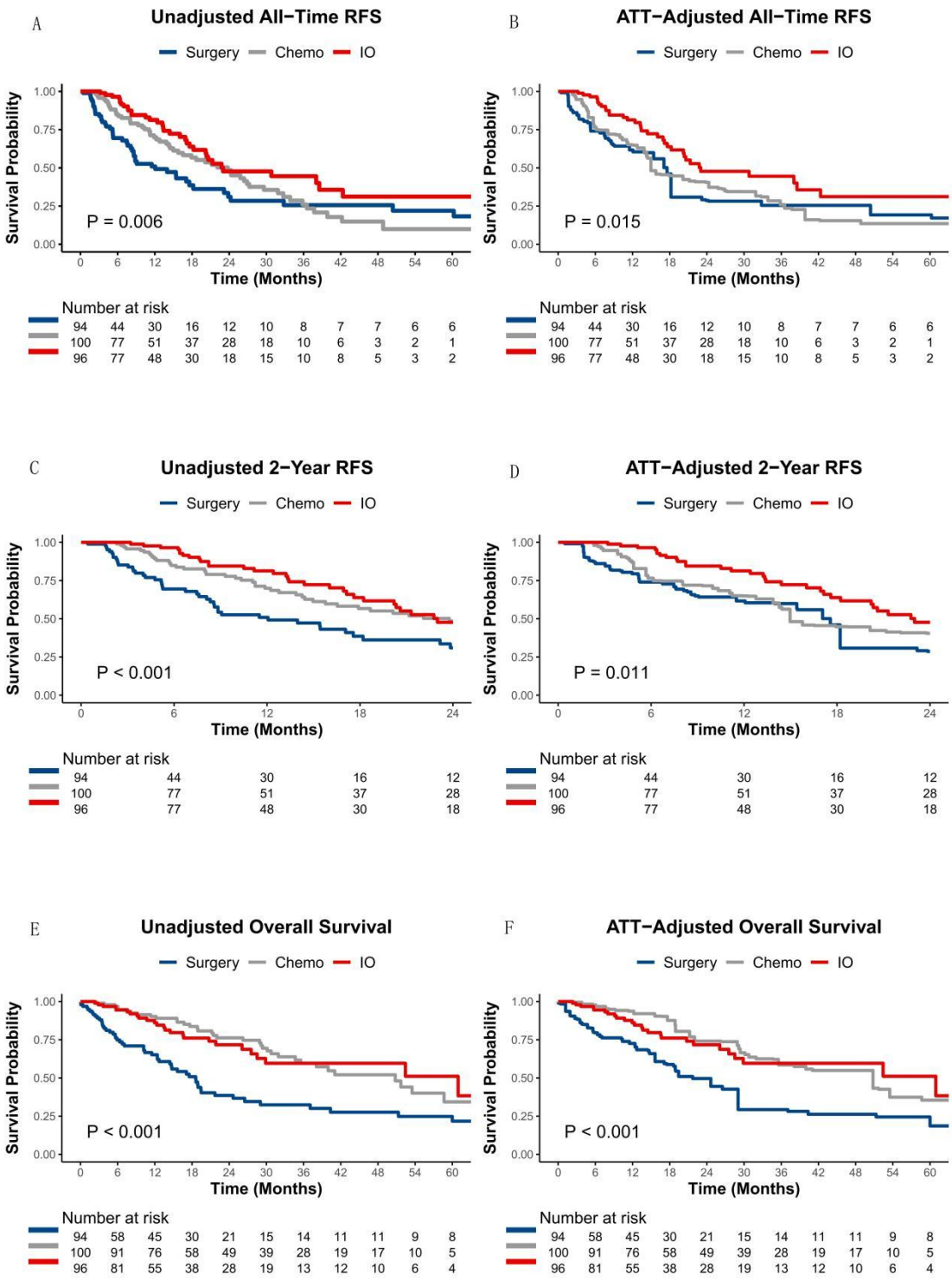


Figure 7 Survival outcomes according to adjuvant treatment strategies before and after IPTW adjustment. A, B Kaplan-Meier curves comparing all-time recurrence-free survival (RFS) among the surgery alone, adjuvant chemotherapy, and

adjuvant chemoimmunotherapy groups in the unadjusted (**A**) and IPTW-adjusted (**B**) cohorts. **C, D** Kaplan-Meier curves for 2-year RFS in the unadjusted (**C**) and IPTW-adjusted (**D**) cohorts. **E, F** Kaplan-Meier curves for overall survival (OS) in the unadjusted (**E**) and IPTW-adjusted (**F**) cohorts. The *P* values in the adjusted cohorts were derived from the doubly robust Cox proportional hazards regression model to account for residual confounding. Abbreviations: IPTW, inverse probability of treatment weighting; RFS, recurrence-free survival; OS, overall survival.

With respect to overall survival (OS), both adjuvant chemotherapy (HR = 0.381; 95% CI, 0.209–0.697; *P* = .002) and adjuvant chemoimmunotherapy (HR = 0.474; 95% CI, 0.274–0.820; *P* = .008) were associated with significantly improved survival relative to surgery alone. However, the hazard ratios for the two adjuvant groups were comparable, with widely overlapping 95% confidence intervals, OS did not differ significantly between the two adjuvant groups. (Figures 7E–F, Table 4).

TABLE 4. Doubly Robust Cox Proportional Hazards Regression Analysis for RFS and OS in the IPTW-Adjusted Cohort

Variables	All-Time RFS		2-Year RFS		Overall Survival	
	HR (95% CI)	P	HR (95% CI)	P	HR (95% CI)	P
Treatment Group						
Surgery alone	Reference		Reference		Reference	

Adjuvant Chemo	0.884 (0.516 - 1.510)	0.652	0.774 (0.437 - 1.370)	0.378	0.381 (0.209 - 0.697)	0.002
Immuno-Chemo	0.505 (0.315 - 0.812)	0.005	0.466 (0.286 - 0.758)	0.002	0.474 (0.274 - 0.820)	0.008
Tumor multiplicity						
Single	Reference		Reference		Reference	
Multiple	1.840 (1.060 - 3.200)	0.031	1.710 (0.981 - 2.990)	0.059	1.490 (0.895 - 2.480)	0.125
Tumor size, cm	1.090 (1.010 - 1.180)	0.032	1.080 (0.983 - 1.180)	0.111	1.050 (0.974 - 1.130)	0.204
Albumin, g/L	1.010 (0.961 - 1.060)	0.744	1.010 (0.955 - 1.060)	0.792	0.901 (0.838 - 0.968)	0.004
SII	1.000 (1.000 - 1.000)	0.344	1.000 (1.000 - 1.000)	0.656	1.000 (1.000 - 1.000)	0.442
CA 19-9, U/mL	1.000 (1.000 - 1.000)	0.067	1.000 (1.000 - 1.000)	0.062	1.000 (1.000 - 1.000)	0.434
Differentiation grade						
Well to moderate	Reference		Reference		Reference	
Poor to undifferentiated	1.660 (1.060 - 2.580)	0.025	1.640 (1.010 - 2.660)	0.043	1.470 (0.871 - 2.460)	0.150
Resection margin						
R0	Reference		Reference		Reference	
R1	1.650 (1.030 - 2.650)	0.039	1.440 (0.824 - 2.520)	0.200	1.530 (0.921 - 2.530)	0.101
Lymph node metastasis						
N0	Reference		Reference		Reference	
N+	1.300 (0.830 - 2.020)	0.254	1.430 (0.867 - 2.360)	0.161	1.790 (1.130 - 2.850)	0.013
Microvascular invasion						
No	Reference		Reference		Reference	

Yes	1.230 (0.781 - 1.950)	0.368	1.310 (0.795 - 2.160)	0.289	2.580 (1.480 - 4.510)	0.001
Macrovascular invasion						
No	Reference		Reference		Reference	
Yes	0.648 (0.376 - 1.120)	0.117	0.603 (0.332 - 1.100)	0.097	0.892 (0.566 - 1.410)	0.623
Hepatolithiasis						
No	Reference		Reference		Reference	
Yes	1.520 (0.970 - 2.370)	0.068	1.600 (0.997 - 2.560)	0.051	1.940 (1.200 - 3.130)	0.006

412 The model was adjusted for age, histologic grade, resection margin, lymph node
413 status, tumor multiplicity, tumor size, macrovascular invasion, and microvascular
414 invasion. HRs with 95% CIs and P values are reported.
415 Abbreviations: RFS, recurrence-free survival; OS, overall survival; HR, hazard ratio;
416 CI, confidence interval; IPTW, inverse probability of treatment weighting; ATT,
417 average treatment effect on the treated; Chemo, adjuvant chemotherapy; Immuno-
418 Chemo, adjuvant chemoimmunotherapy.
419
420 The robustness of these findings was assessed in a pre-specified sensitivity analysis
421 using ATO weighting. The ATO-weighted analysis yielded effect estimates consistent
422 with the primary ATT analysis for the key endpoint of 2-year RFS, with adjuvant
423 chemoimmunotherapy remaining significantly associated with reduced recurrence risk
424 compared with surgery alone (HR = 0.568; 95% CI, 0.332–0.973; P = 0.039). The all-

time RFS estimate was directionally consistent but attenuated (HR = 0.642; P = 0.091). Full results are presented in Additional file 1: Supplementary Table 1. Further adjustment for year of surgery (≤2020 vs. >2020) to account for potential temporal confounding also yielded consistent results, with adjuvant chemoimmunotherapy remaining significantly associated with reduced 2-year recurrence risk (HR = 0.51; 95% CI, 0.29–0.90; P = 0.019).Prespecified exploratory subgroup analyses for the primary endpoint of 2-year RFS demonstrated a directionally consistent benefit of adjuvant chemoimmunotherapy over surgery alone across all evaluated subgroups, with no statistically significant interactions observed for age, sex, histological grade, lymph node status, or resection margin status (all P for interaction > 0.05; Additional file 2: Supplementary Figure 1). A significant interaction was noted for tumor location (P for interaction = 0.005), driven by an imprecise estimate in the distal cholangiocarcinoma subgroup (HR, 2.81; 95% CI, 0.40–20.00; n = 44), likely attributable to the very small sample size and resulting statistical instability. The RFS benefit appeared particularly pronounced in patients with poorly differentiated tumors (HR, 0.35; P = 0.010), node-positive disease (HR, 0.40; P = 0.006), and R1 resection margins (HR, 0.15; P = 0.028).

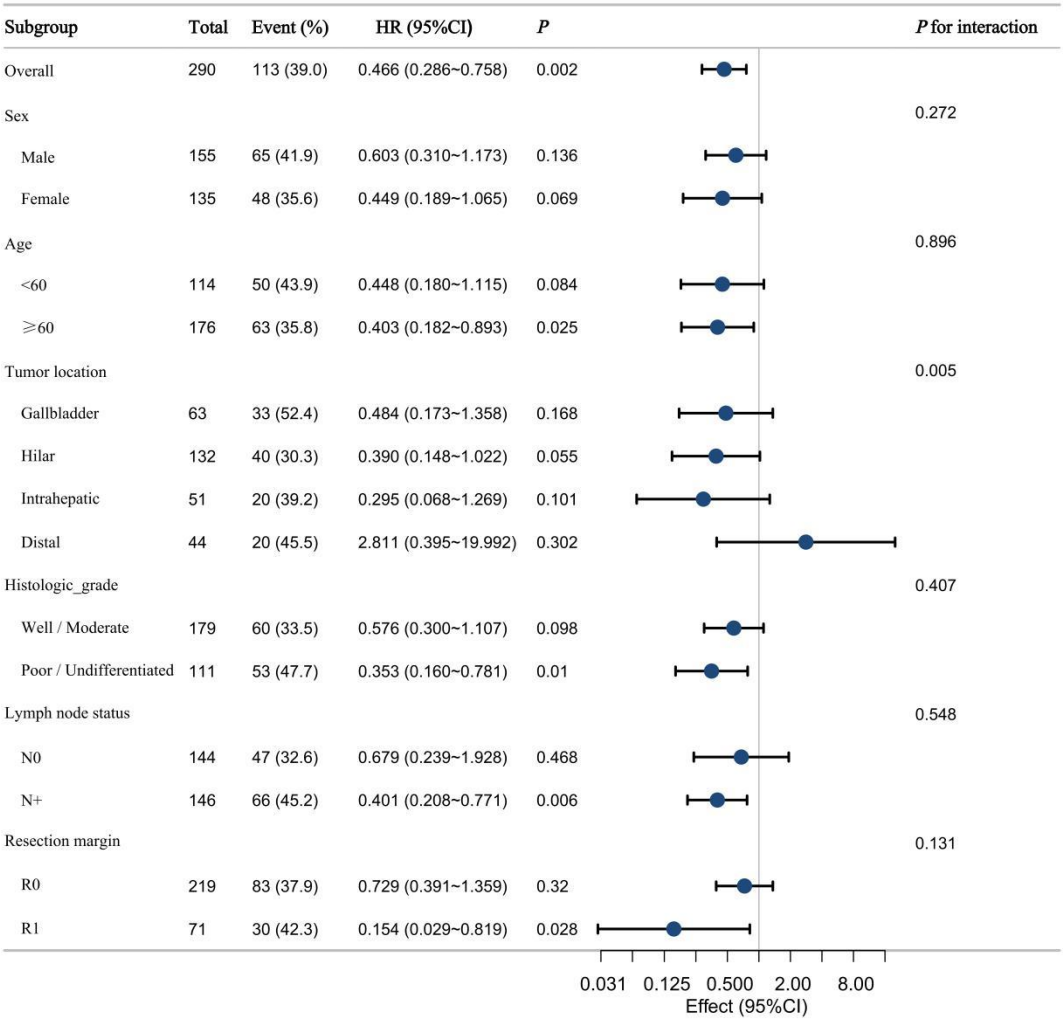
Supplementary Table S1 Sensitivity Analysis of Treatment Effect Estimates Using ATO Weighting

Outcome	Comparison		Primary Analysis (ATT)		Sensitivity 1: ATO Weighting		Sensitivity 2: ATT + Year of Surgery	
			HR (95% CI)	P	HR (95% CI)	P	HR (95% CI)	P
2-Year RFS	Chemo vs Surgery		0.77 (0.44 – 1.37)	0.378	0.71 (0.43 – 1.18)	0.191	0.97 (0.50 – 1.86)	0.918
	IO vs Surgery		**0.47 (0.29 – 0.76)**	**0.002**	**0.57 (0.33 – 0.97)**	**0.039**	**0.51 (0.29 – 0.90)**	**0.019**
All-Time RFS	Chemo vs Surgery		0.88 (0.52 – 1.51)	0.652	0.88 (0.54 – 1.42)	0.598	1.10 (0.61 – 1.99)	0.756
	IO vs Surgery		0.51 (0.32 – 0.81)	0.005	0.64 (0.38 – 1.07)	0.091	0.53 (0.31 – 0.91)	0.020
Overall Survival	Chemo vs Surgery		0.38 (0.21 – 0.70)	0.002	0.43 (0.26 – 0.70)	0.001	0.30 (0.14 – 0.62)	0.001
	IO vs Surgery		0.47 (0.27 – 0.82)	0.008	0.51 (0.29 – 0.91)	0.022	0.40 (0.21 – 0.76)	0.005

Abbreviations: ATT, average treatment effect on the treated; ATO, average treatment effect on the overlap; RFS, recurrence-free survival; OS, overall survival; HR, hazard ratio; CI, confidence interval; Chemo, adjuvant chemotherapy; IO, adjuvant chemoimmunotherapy.

Notes: All estimates were derived from doubly robust Cox proportional hazards models. The primary analysis used ATT weighting with the chemoimmunotherapy group as the target. Sensitivity 1 used ATO weighting, which restricts the estimand to the region of clinical equipoise. Sensitivity 2 retained ATT weighting but additionally included year of surgery (≤2020 vs. >2020) as a covariate in both the propensity score

and doubly robust models to account for potential temporal confounding. All models adjusted for age, histologic grade, resection margin, lymph node status, and the principal determinants of pathological T stage. Bold rows indicate the primary efficacy comparison of interest.



Supplementary Figure S1 Subgroup analysis of recurrence-free survival. Forest plot detailing the hazard ratios (HRs) and 95% confidence intervals (CIs) of the adjuvant treatment effect across prespecified clinical subgroups. The overall HR

463 corresponds to the comparison between the adjuvant chemoimmunotherapy and
464 surgery alone groups. The *P* for interaction evaluates whether the treatment benefit
465 varies significantly across different patient strata. *Abbreviations:* HR, hazard ratio; CI,
466 confidence interval.
467
468
469 **Safety and Tolerability**
470 In addition to survival outcomes, the safety and tolerability profiles of patients
471 receiving systemic therapy (adjuvant chemotherapy, n = 100; adjuvant
472 chemoimmunotherapy, n = 96) were compared. The incidence of any-grade treatment-
473 related adverse events (TRAEs) was higher in the chemoimmunotherapy group than
474 in the chemotherapy alone group (28.1% vs. 14.0%). Notably, the incidence of grade
475 ≥3 TRAEs—defined as severe or medically significant events—was 12.5% (12/96) in
476 the chemoimmunotherapy group, significantly higher than the 2.0% (2/100) observed
477 in the chemotherapy group (*P* = .005).
478 The excess severe adverse events in the chemoimmunotherapy group were primarily
479 attributable to hematologic toxicity. Specifically, the incidence of grade ≥3
480 thrombocytopenia was significantly higher in the chemoimmunotherapy group
481 compared with the chemotherapy group (5.2% vs. 0.0%; *P* = .027). With respect to

482 immune-related adverse events (irAEs), three cases of hypothyroidism were
483 documented in the chemoimmunotherapy group; all were mild (grade 1–2) and
484 effectively managed with hormone replacement therapy.
485 These findings indicate that although the addition of immunotherapy to adjuvant
486 chemotherapy was associated with an increased incidence of adverse events—
487 primarily myelosuppression—the overall safety profile of the adjuvant
488 chemoimmunotherapy regimen remains manageable and acceptable under rigorous
489 clinical monitoring and appropriate supportive care (Table 5).
490
491 **Table 5 Treatment-Related Adverse Events in the As-Treated Population.**

Adverse Events	Adjuvant Chemotherapy (n = 100)		Adjuvant Immuno-Chemotherapy (n = 96)		*P* value (Grade ≥ 3)
	Any Grade, n (%)	Grade ≥ 3, n (%)	Any Grade, n (%)	Grade ≥ 3, n (%)	
Overall TRAEs	14 (14.0%)	2 (2.0%)	27 (28.1%)	12 (12.5%)	0.005
Hematologic toxicities					
Anemia	4 (4.0%)	1 (1.0%)	13 (13.5%)	3 (3.1%)	0.361
Lymphopenia	3 (3.0%)	0 (0.0%)	12 (12.5%)	2 (2.1%)	0.239
Thrombocytope-nia	3 (3.0%)	0 (0.0%)	10 (10.4%)	5 (5.2%)	0.027
Neutropenia	3 (3.0%)	0 (0.0%)	4 (4.2%)	2 (2.1%)	0.239
Hepatic and metabolic toxicities					

Adverse Events	Adjuvant Chemotherapy (n = 100)		Adjuvant Immuno-Chemotherapy (n = 96)		*P* value (Grade ≥ 3)
	Any Grade, n (%)	Grade ≥ 3, n (%)	Any Grade, n (%)	Grade ≥ 3, n (%)	
Hypoalbuminemia	2 (2.0%)	0 (0.0%)	12 (12.5%)	1 (1.0%)	0.49
AST increased	0 (0.0%)	0 (0.0%)	3 (3.1%)	1 (1.0%)	0.49
ALT increased	0 (0.0%)	0 (0.0%)	2 (2.1%)	0 (0.0%)	-
Hyperbilirubinemia	0 (0.0%)	0 (0.0%)	3 (3.1%)	2 (2.1%)	0.239
Amylase / ALP increased	1 (1.0%)	0 (0.0%)	1 (1.0%)	1 (1.0%)	0.49
Gastrointestinal and other toxicities					
Hypertension	1 (1.0%)	1 (1.0%)	3 (3.1%)	1 (1.0%)	> 0.99
Nausea / Vomiting	1 (1.0%)	0 (0.0%)	3 (3.1%)	1 (1.0%)	0.49
Decreased appetite / Abdominal pain	3 (3.0%)	0 (0.0%)	0 (0.0%)	0 (0.0%)	-
immune-related adverse events (irAEs)					
Hypothyroidism	0 (0.0%)	0 (0.0%)	3 (3.1%)	0 (0.0%)	-
Rash	2 (2.0%)	0 (0.0%)	0 (0.0%)	0 (0.0%)	-

P values were calculated using Fisher's exact test for between-group comparisons of grade ≥3 adverse events. Dashes indicate that no grade ≥3 events were observed in either group.

Abbreviations: TRAEs, treatment-related adverse events; AST, aspartate aminotransferase; ALT, alanine aminotransferase; ALP, alkaline phosphatase; irAEs, immune-related adverse events.

Discussion

Principal Findings

This multicenter real-world study of high-risk biliary tract cancer (BTC) patients undergoing curative-intent resection yielded two principal findings. First, an individualized nomogram integrating local tumor burden (LODDS) and host systemic inflammatory status (SII, albumin) with conventional clinicopathological variables demonstrated good discriminatory performance for predicting 1-year and moderate performance for 2-year recurrence-free survival (RFS) (AUC = 0.829 and 0.709, respectively). Second, in the high-risk population defined by this model, adjuvant chemoimmunotherapy was associated with a 53.4% reduction in the risk of 2-year early recurrence compared with surgery alone (HR = 0.466; 95% CI, 0.286–0.758; P = 0.002), a benefit that was not observed with adjuvant chemotherapy alone (HR = 0.774 for 2-year RFS; P = 0.378). These findings suggest a potential paradigm shift in the postoperative management of high-risk BTC—from a singular focus on prolonging overall survival (OS) toward the dual objectives of preventing early recurrence while maintaining long-term survival benefit.

Value of the Multidimensional Prediction Model

A central contribution of this study is the integration of previously isolated prognostic biomarkers into a single, clinically actionable nomogram. While prior studies have independently demonstrated the prognostic value of LODDS in mitigating stage migration[11-13] and SII as a reflection of host immune-inflammatory dysregulation[16, 17], these markers have rarely been combined within a machine learning-driven framework. By employing LASSO regression for high-dimensional feature selection, the current model captured the complementary information provided by local pathological burden (LODDS, HR = 1.30; $P < 0.001$) and systemic microenvironmental status (SII, albumin), thereby improving upon the granularity of risk stratification achievable with the AJCC TNM staging system alone. Notably, the model retained discriminative performance after rigorous internal validation with 1,000 bootstrap resamples (1-year AUC = 0.829; 2-year AUC = 0.709), and decision curve analysis confirmed net clinical benefit across a wide range of threshold probabilities. However, direct comparison with previously published BTC prognostic models is limited by differences in patient populations and endpoints; future external validation in independent cohorts is required to establish the generalizability of this nomogram.

Efficacy of Adjuvant Chemoimmunotherapy in the High-Risk Setting

This study provides novel real-world evidence supporting the extension of chemoimmunotherapy—established as standard of care in advanced BTC by the

TOPAZ-1 and KEYNOTE-966 trials[7, 8]—into the postoperative adjuvant setting for high-risk patients. Using doubly robust estimation within an IPTW-balanced pseudo-randomized framework, we observed that adjuvant chemoimmunotherapy significantly reduced early recurrence risk, whereas adjuvant chemotherapy alone did not (HR for chemotherapy vs. surgery alone = 0.884; 95% CI, 0.516–1.510; P = 0.652). This divergence in efficacy aligns with the notion that traditional cytotoxic chemotherapy, even when delivered as recommended by the BILCAP trial[5], may have inherent limitations in controlling minimal residual disease (MRD) in BTC.

From a safety standpoint, the adjuvant chemoimmunotherapy regimen was associated with a significantly higher incidence of grade ≥3 treatment-related adverse events compared with chemotherapy alone (12.5% vs. 2.0%; P = 0.005), primarily driven by hematologic toxicity, particularly thrombocytopenia (5.2% vs. 0%; P = 0.027). Nevertheless, the overall toxicity profile appeared manageable and consistent with the known safety profiles of PD-1/PD-L1 inhibitors combined with chemotherapy. Immune-related adverse events were infrequent and mild, with only three cases of grade 1–2 hypothyroidism documented, all effectively managed with hormone replacement therapy.

Mechanisms Underlying the Differential Efficacy of Chemoimmunotherapy versus Chemotherapy Alone

The superior recurrence-prevention capacity of adjuvant chemoimmunotherapy over chemotherapy alone can be understood through the unique tumor microenvironment of BTC. BTC is characterized by a prominent desmoplastic stroma[10], in which cancer-associated fibroblasts (CAFs) deposit abundant extracellular matrix (ECM) that elevates interstitial fluid pressure and impedes the penetration of cytotoxic agents[18]. Moreover, the dense stroma and sparse lymphocytic infiltration render BTC an immune "cold" tumor, explaining the low response rates to single-agent immune checkpoint blockade[19]. The addition of cytotoxic chemotherapy to immunotherapy generates a synergistic effect: chemotherapy induces immunogenic cell death (ICD), characterized by the release of damage-associated molecular patterns (DAMPs) such as calreticulin, ATP, and HMGB1, which in turn promotes the uptake and presentation of previously occult tumor neoantigens by dendritic cells. This acts as an in situ vaccine, priming and activating CD8+ cytotoxic T lymphocytes[20]. Concurrent PD-1/PD-L1 blockade then alleviates the immunosuppressive signals that would otherwise dampen this nascent immune response, effectively converting the "cold" tumor microenvironment into a "hot" one capable of eliminating MRD. This mechanistic synergy, operating at the intersection of direct tumor cell kill and adaptive immune reactivation, plausibly explains why chemoimmunotherapy substantially reduced early recurrence risk while chemotherapy alone did not.

Interpretation of the Overall Survival Results

Despite the significant RFS benefit, we observed no statistically significant difference in OS between the adjuvant chemoimmunotherapy and adjuvant chemotherapy groups (HR = 0.474 vs. 0.381, with widely overlapping confidence intervals). Several factors may account for this apparent discrepancy. First, the dilution effect of post-progression survival (PPS) is likely substantial[21]. With the expanding armamentarium of effective later-line therapies—including immunotherapy rechallenge, targeted agents, and locoregional ablation—patients who experience early recurrence after adjuvant chemotherapy alone may still achieve meaningful survival prolongation, thereby compressing the OS difference. Second, the sample size was not powered to detect modest OS differences, and the number of OS events may not have reached maturity at the data cutoff. Third, the reduction in effective sample size after IPTW weighting (ESS = 43.2 and 43.3 for the surgery and chemotherapy groups, respectively) further limited statistical precision for the OS comparison. It is important to emphasize, however, that from a patient-centered perspective, prolonging recurrence-free survival is an intrinsically valuable outcome: it delays symptom burden, preserves quality of life, and reduces subsequent reliance on salvage therapies. The core clinical value of adjuvant chemoimmunotherapy, therefore, lies not in an OS advantage that may require years of

follow-up to manifest, but in the immediate translation of a reduction in early recurrence risk into extended disease-free time.

Limitations

Several limitations warrant careful consideration. First, this was a retrospective study conducted at a single center, and despite the use of IPTW and doubly robust regression, residual confounding from unmeasured variables (e.g., subtle variations in surgical technique, host genetic background) cannot be fully excluded[22]. Second, the effective sample sizes for the surgery alone and adjuvant chemotherapy groups were substantially reduced after ATT weighting (ESS = 43.2 and 43.3), which may have limited the precision of intergroup comparisons. Third, the nomogram underwent internal validation only; its generalizability must be confirmed in independent, prospectively collected multicenter cohorts[23]. Fourth, the chemoimmunotherapy regimen encompassed heterogeneous chemotherapy backbones and PD-1/PD-L1 agents, precluding subgroup analyses to identify the optimal combination. Fifth, to avoid potential endogeneity introduced by variations in surgical lymph node yield, the propensity score model incorporated binary lymph node status (N0 vs. N+) rather than the continuous LODDS. LODDS was used exclusively in the nomogram and as a descriptive variable in baseline comparisons, not as a weighting covariate. Sixth, residual imbalance persisted for hepatolithiasis (SMD = 0.204) and

pT stage (SMD = 0.288) after weighting, although these variables were adjusted for in the doubly robust model. Reassuringly, a pre-specified sensitivity analysis using ATO weighting—which is less susceptible to extreme propensity score weights—yielded effect estimates consistent with the primary ATT analysis for the 2-year RFS endpoint (HR = 0.568; P = 0.039; Additional file 1: Supplementary Table 1), supporting the robustness of the primary findings to the choice of weighting strategy. Additionally, exploratory subgroup analyses demonstrated directionally consistent RFS benefits across all prespecified subgroups, with no significant interactions for age, sex, histological grade, lymph node status, or resection margin status (all P for interaction > 0.05; Additional file 2: Supplementary Figure 1). A nominally significant interaction was observed for tumor location (P for interaction = 0.005), driven by an imprecise estimate in the distal cholangiocarcinoma subgroup (n = 44) that likely reflects statistical instability due to the very small sample size.

Future Directions

Building on these findings, several research priorities emerge. First, prospective randomized controlled trials are warranted to provide definitive evidence for adjuvant chemoimmunotherapy in high-risk BTC. Second, external validation of the nomogram across diverse geographic and clinical settings is essential before its routine clinical adoption. Third, future iterations of this prognostic model should incorporate molecular

biomarkers—such as circulating tumor DNA (ctDNA) dynamics, FGFR2 fusions, and IDH1/2 mutations[24]—to shift from macroscopic risk stratification toward molecularly informed precision surveillance. Finally, the web-based calculator developed in this study should be validated across diverse clinical settings.

Conclusions

This study constructed and internally validated a multidimensional predictive model that integrates local tumor burden (LODDS) with systemic immune-inflammatory status (SII and albumin), enabling precise, individualized estimation of early postoperative recurrence risk in high-risk biliary tract cancer (BTC). Furthermore, advanced causal inference analysis confirmed that adjuvant chemoimmunotherapy confers a significant reduction in 2-year recurrence risk in real-world clinical practice. Although no statistically significant difference in overall survival (OS) was observed, adjuvant chemoimmunotherapy demonstrated considerable clinical value in intercepting early recurrence and prolonging disease-free survival. Collectively, these findings provide a promising tool for precise risk stratification of high-risk BTC patients and offer critical evidence to inform the optimization of postoperative management strategies, addressing key limitations of traditional adjuvant approaches.

Supplementary Information

Additional file 1

Format: .docx

Title: Supplementary Table S1.

Description: Sensitivity analysis of treatment effect estimates using average treatment effect on the overlap (ATO) weighting and further adjustment for the year of surgery.

Additional file 2

Format: .pdf

Title: Supplementary Figure 1.

Description: Subgroup analysis of 2-year recurrence-free survival across prespecified clinical characteristics.

Abbreviations

AJCC: American Joint Committee on Cancer; ATO: Average treatment effect on the overlap; ATT: Average treatment effect on the treated; AUC: Area under the curve; BTC: Biliary tract cancer; CA 19-9: Carbohydrate antigen 19-9; CAF: Cancer-associated fibroblast; CI: Confidence interval; CRediT: Contributor Roles Taxonomy; DAMP: Damage-associated molecular pattern; DCA: Decision curve analysis; ECM: Extracellular matrix; EMR: Electronic medical record; ESS: Effective sample size; GBC: Gallbladder cancer; HBsAg: Hepatitis B surface antigen; HR: Hazard ratio; ICD: Immunogenic cell death; ICI: Immune checkpoint inhibitor; ICC: Intrahepatic cholangiocarcinoma; IPTW: Inverse probability of treatment weighting; IQR: Interquartile range; irAE: Immune-related adverse event; LASSO: Least absolute shrinkage and selection operator; LIS: Laboratory information system; LODDS: Log odds of positive lymph nodes; MRD: Minimal residual disease; OS: Overall survival; PD-1: Programmed cell death protein 1; PD-L1: Programmed death ligand 1; PNI:

673 Perineural invasion; PPS: Post-progression survival; RFS: Recurrence-free survival;
674 RCT: Randomized controlled trial; ROC: Receiver operating characteristic; SII:
675 Systemic immune-inflammation index; SMD: Standardized mean difference; TNM:
676 Tumor-node-metastasis; TRAE: Treatment-related adverse event

677

678

679 **Declarations**

680 **Ethics approval and consent to participate**

681 This study was approved by the Institutional Review Board of Sun Yat-sen Memorial
682 Hospital, Sun Yat-sen University. All procedures were performed in accordance with
683 the ethical standards of the 1964 Declaration of Helsinki and its later amendments.
684 Due to the retrospective nature of the study, the requirement for individual informed
685 consent was waived by the IRB. All patient data were anonymized prior to analysis.

686 **Consent for publication**

687 Not applicable.

688 **Availability of data and materials**

689 The datasets used in this study are available from the corresponding author upon
690 reasonable request. However, these data are not publicly available due to
691 considerations regarding patient privacy.

692 **Competing interests**

693 The authors declare that they have no competing interests.

Funding

This research did not receive any specific grant from funding agencies in the public, commercial, or not-for-profit sectors.

Authors' contributions

J.L.: study design and protocol, data extraction, statistical analyses, interpretation of the results, and drafting the article; X.X.: data extraction, statistical analyses; Y.L.: statistical analyses and interpretation of the results; J.H.: data extraction, statistical analyses; L.Z.: study design and protocol, interpretation of the results, and drafting the article. All authors have read and agreed to the published version of the manuscript.

Acknowledgements

Not applicable.

References

1. Ouyang G, Liu Q, Wu Y, Liu Z, Lu W, Li S, et al. The global, regional, and national burden of gallbladder and biliary tract cancer and its attributable risk factors in 195 countries and territories, 1990 to 2017: A systematic analysis for the Global Burden of Disease Study 2017. Cancer. 2021;127(13):2238-50.

2. Groot Koerkamp B, Wiggers JK, Allen PJ, Besselink MG, Blumgart LH, Busch OR, et al. Recurrence Rate and Pattern of Perihilar Cholangiocarcinoma after Curative Intent Resection. J Am Coll Surg. 2015;221(6):1041-9.

713 3. Ebata T, Hirano S, Konishi M, Uesaka K, Tsuchiya Y, Ohtsuka M, et al.
714 Randomized clinical trial of adjuvant gemcitabine chemotherapy versus observation
715 in resected bile duct cancer. Br J Surg. 2018;105(3):192-202.
716 4. Edeline J, Benabdelghani M, Bertaut A, Watelet J, Hammel P, Joly JP, et al.
717 Gemcitabine and Oxaliplatin Chemotherapy or Surveillance in Resected Biliary Tract
718 Cancer (PRODIGE 12-ACCORD 18-UNICANCER GI): A Randomized Phase III
719 Study. J Clin Oncol. 2019;37(8):658-67.
720 5. Primrose JN, Fox RP, Palmer DH, Malik HZ, Prasad R, Mirza D, et al.
721 Capecitabine compared with observation in resected biliary tract cancer (BILCAP): a
722 randomised, controlled, multicentre, phase 3 study. Lancet Oncol. 2019;20(5):663-73.
723 6. Bridgewater J, Fletcher P, Palmer DH, Malik HZ, Prasad R, Mirza D, et al.
724 Long-Term Outcomes and Exploratory Analyses of the Randomized Phase III
725 BILCAP Study. J Clin Oncol. 2022;40(18):2048-57.
726 7. Oh DY, Ruth He A, Qin S, Chen LT, Okusaka T, Vogel A, et al. Durvalumab
727 plus Gemcitabine and Cisplatin in Advanced Biliary Tract Cancer. NEJM Evid.
728 2022;1(8):EVIDoa2200015.
729 8. Kelley RK, Ueno M, Yoo C, Finn RS, Furuse J, Ren Z, et al. Pembrolizumab
730 in combination with gemcitabine and cisplatin compared with gemcitabine and
731 cisplatin alone for patients with advanced biliary tract cancer (KEYNOTE-966): a

732 randomised, double-blind, placebo-controlled, phase 3 trial. Lancet.
733 2023;401(10391):1853-65.
734 9. Xiao H, Ji J, Li S, Lai J, Wei G, Wu J, et al. Adjuvant Chemoradiation and
735 Immunotherapy for Extrahepatic Cholangiocarcinoma and Gallbladder Cancer: A
736 Randomized Clinical Trial. JAMA Oncol. 2025;11(9):1021-9.
737 10. Banales JM, Marin JJG, Lamarca A, Rodrigues PM, Khan SA, Roberts LR, et
738 al. Cholangiocarcinoma 2020: the next horizon in mechanisms and management. Nat
739 Rev Gastroenterol Hepatol. 2020;17(9):557-88.
740 11. Amini N, Spolverato G, Kim Y, Gupta R, Margonis GA, Ejaz A, et al. Lymph
741 node status after resection for gallbladder adenocarcinoma: prognostic implications of
742 different nodal staging/scoring systems. J Surg Oncol. 2015;111(3):299-305.
743 12. Li R, Lu Z, Sun Z, Shi X, Li Z, Shao W, et al. A Nomogram Based on the Log
744 Odds of Positive Lymph Nodes Predicts the Prognosis of Patients With Distal
745 Cholangiocarcinoma After Surgery. Front Surg. 2021;8:757552.
746 13. Conci S, Ruzzenente A, Sandri M, Bertuzzo F, Campagnaro T, Bagante F, et
747 al. What is the most accurate lymph node staging method for perihilar
748 cholangiocarcinoma? Comparison of UICC/AJCC pN stage, number of metastatic
749 lymph nodes, lymph node ratio, and log odds of metastatic lymph nodes. Eur J Surg
750 Oncol. 2017;43(4):743-50.

14. Terasaki F, Sugiura T, Okamura Y, Ito T, Yamamoto Y, Ashida R, et al. Systemic immune-inflammation index as a prognostic marker for distal cholangiocarcinoma. Surg Today. 2021;51(10):1602-9.

15. Tibshirani R. Regression Shrinkage and Selection Via the Lasso. Journal of the Royal Statistical Society: Series B (Methodological). 2018;58(1):267-88.

16. Hu B, Yang XR, Xu Y, Sun YF, Sun C, Guo W, et al. Systemic immune-inflammation index predicts prognosis of patients after curative resection for hepatocellular carcinoma. Clin Cancer Res. 2014;20(23):6212-22.

17. Abdulrazzak M, Björkhem-Bergman L, Villard C, Gerling M, Gustavell T, Jansson H. Hypoalbuminemia as a prognostic marker for survival in biliary tract cancer: associations with tumor type, treatment and sex. J Cancer Res Clin Oncol. 2026;152(1):36.

18. Fabris L, Sato K, Alpini G, Strazzabosco M. The Tumor Microenvironment in Cholangiocarcinoma Progression. Hepatology. 2021;73 Suppl 1(Suppl 1):75-85.

19. Rizzo A, Ricci AD, Brandi G. PD-L1, TMB, MSI, and Other Predictors of Response to Immune Checkpoint Inhibitors in Biliary Tract Cancer. Cancers (Basel). 2021;13(3).

20. Galluzzi L, Humeau J, Buqué A, Zitvogel L, Kroemer G. Immunostimulation with chemotherapy in the era of immune checkpoint inhibitors. Nat Rev Clin Oncol. 2020;17(12):725-41.

21. Broglio KR, Berry DA. Detecting an overall survival benefit that is derived from progression-free survival. J Natl Cancer Inst. 2009;101(23):1642-9.

22. Austin PC. An Introduction to Propensity Score Methods for Reducing the Effects of Confounding in Observational Studies. Multivariate Behav Res. 2011;46(3):399-424.

23. Collins GS, Reitsma JB, Altman DG, Moons KG. Transparent Reporting of a multivariable prediction model for Individual Prognosis or Diagnosis (TRIPOD): the TRIPOD statement. Ann Intern Med. 2015;162(1):55-63.

24. Yu J, He AR, Ouf M, Mehta R, Anaya DA, Denbo J, et al. Detecting Early Recurrence With Circulating Tumor DNA in Stage I-III Biliary Tract Cancer After Curative Resection. JCO Precis Oncol. 2025;9:e2400443.